

Numerical Simulation of Slurry Flows in Heterogeneous and Saltation Regimes in Horizontal Pipelines

Jaime Gonzalez^{*a}, Nazgul Sabirgalieva^b, Luis Rojas-Solórzano^{b,c}, Gustavo Zarruk^d

^aDepartment of Petroleum Engineering, Escuela Politécnica Nacional, Quito, Ecuador

^bSchool of Engineering, Department of Chemical Engineering, Nazarbayev University, Astana, Kazakhstan

^cFluid Mechanics Laboratory, Simon Bolivar University, Caracas, Venezuela

^dRestrack, Technology and Interpretation, Instituttveien 18, Kjeller, Norway

jaime.gonzalez@epn.edu.ec

Liquid-solid flows, in both heterogeneous and saltation regimes, are critical in the transport of suspended solid particles in pipelines prone to particles settling and accumulating on the bottom of the pipe, eventually blocking the flow and risking flow assurance. Numerical simulation of a statistically developed and steady two-phase liquid-solid flow in a horizontal pipe is performed by solving Reynolds-Averaged Navier-Stokes (RANS) equations within an Eulerian-Eulerian framework to predict the complex interaction among particles and between particles and their transporting fluid and surrounding walls. Particles are treated as a secondary fluid phase with viscosity determined using the Granular Kinetic Theory (GKT), including its three potential contributions, i.e., frictional, collisional and kinetic interactions. A case study for a horizontal pipe flow with mono-disperse and bi-disperse liquid-particle mixtures, at different flow velocities and particle-bulk concentration, is presented. Particles concentration for statistically steady heterogeneous and saltation regimes without a fixed bed are presented. Governing equations for each phase are solved numerically using ANSYS-Fluent platform which is based on the finite volume method to integrate the equations about each control volume and turning the problem into a system of algebraic equations. A second-order spatial discretization is implemented across the model. Bulk concentrations of solid particles in water were considered in percentage of 10% and 20%. Solid particles of 0.125mm and 0.440mm in diameter were used in the study, while bulk velocities of 1m/s, 2m/s and 3m/s were prescribed.

1. Introduction

Transportation of slurries through a pipeline is common in many industrial applications. In most cases, slurry pipelines are more energy efficient, with lower operating and maintenance costs, than any other bulk material handling methods (Ekambara et al., 2009).

The analysis of slurry flows in pipelines entails the consideration of a large number of variables: pipeline orientation, cross-section geometry, wall roughness, particle size, particle-bulk distribution, particle density, particle shape, fluid density, fluid velocity, fluid rheology and properties of the fluid-particle interface.

Due to the wide range of possible scenarios, many studies aim to evaluate restricted range of conditions (Hu, 2006) or to scale down field situations. Experimental results are limited to be used in the understanding of similar cases to those explored in the laboratory due to the difficulty of generating theoretical models that consider all variables and flow regimes. Thus, Computational Fluid Dynamics (CFD) has emerged as a useful and powerful tool, which coupled with benchmark experimental results, permits prediction of unknown or particular slurry flow scenarios. For example, CFD Eulerian-Eulerian models have been used with significant success (Hernandez et al., 2008; Ekambara et al., 2009; Kaushal et al., 2012) in modelling two-phase liquid-particle flows considering both phases as fully interpenetrating continua and the solid-phase viscosity determined using Granular Kinetic Theory (GKT).

The GKT is based on the kinetic theory of gases in a generalized manner to take into account inelastic particle collisions to define a solid-phase granular temperature that affects directly the phase stress tensor. Tuning up

the model requires especial attention to aspects such as: boundary conditions, interphase momentum transfer relationships, coefficients of restitution and the radial distribution function.

In this study, the full three-dimensional Reynolds Averaged Navier-Stokes (RANS) equations in Eulerian–Eulerian framework are used to model the flow of a mixture of sand and water in statistically steady heterogeneous and saltation regimes without a fixed bed. Turbulence was modelled through the standard $k-\epsilon$ differential equations coupled to the RANS. Additionally, the solid phase is modelled in the Eulerian framework as an interpenetrating fluid with viscosity determined by GKT as in previous works (e.g., Hernandez et al., 2008; Ekambara et al., 2009; Kaushal et al., 2012). Concentration and velocity particle profiles are compared with experimental data from Kaushal et al. (2005).

1.1 Background on experimental studies

Durand and Condolios (1952) were the first in classify slurry flows considering settling/non-settling slurries in horizontal pipes based on average particle size. Newitt et al. (1955), Thomas (1964) and other authors modified the original classification of Durand and Condolios, describing four flow regimes: homogeneous flow, heterogeneous flow, saltation flow and stationary bed flow as a function of mean velocity flow, particle diameter and bulk volumetric fraction.

Chemloul et al. (2009) and Polansky (2014) through different experimental procedures and devices such as Pulsed Ultrasonic Doppler Velocimetry PUDV and Electrical Resistance Tomography (ERT), measured simultaneously the local velocity and the local concentration in a solid-liquid suspension flowing through a horizontal pipe and confirmed that the cross-section solids distribution responds to the slip velocity, particle properties, flow velocity and bulk concentration.

Wasp et al. (1979), Wilson and Pugh (1988) and Gillies and Shook (2000) derived a correlation between pressure drop and solids density, liquid density, particle size, solids concentration, pipe diameter, viscosity of flowing media and flow velocity in solid-liquid flows, but still limited to particular scenarios.

From the literature review it was also quite clear that cross-section concentration profiles have profound effect on pressure drop in slurry flows.

1.2 Background on numerical studies

In the past, numerical simulations have been performed for slurry flows in horizontal pipe with relative success in predicting flow properties such as: particle concentration, slip velocity, velocity profile for each phase and pressure drop. Ling et al. (2003) introduced a simplified 3D Algebraic Slip Mixture (ASM) model. The key aspect in Ling et al.'s model is the way the slip velocity between phases is obtained. Hernandez et al. (2008), Ekambara et al. (2009), Kaushal et al. (2012), Kumar et al. (2015) and Ofei and Ismail (2016) developed their simulations focusing on Eulerian-Eulerian framework to model the flow of a mixture of sand particles and water in a horizontal pipe. Homogeneous and heterogeneous flow regimes were considered in their works. Most authors developed their simulations using $k-\epsilon$ turbulence model and the control volume method to solve the governing equations in ANSYS-CFD platform. Additionally, closure of solid-phase momentum equations required a description of the solid-phase stress tensor, for which constitutive relations for the solid-phase stress considering the inelastic nature of particle collisions based on the GKT concepts were used. Nevertheless, Hernandez et al. (2008), Ekambara et al. (2009) and Ofei and Ismail (2016) only considered the kinetic and collisional contributions of the solid-phase viscosity. Furthermore, Kaushal et al. (2012) simulated fine particles (0.125mm) at high concentration (50%) and Kumar et al. (2015) modelled pressure drop in a 90-degree horizontal pipe bend with radius of 148 mm and pipe diameter of 53 mm.

2. Mathematical modelling

An Eulerian-Eulerian approach in which two phases are considered to be interpenetrating continua is implemented using ANSYS Fluent v.15.0 platform.

The full three-component GKT model is used to compute the solid-phase granular viscosity. Particles are considered to be smooth, spherical and inelastic, undergoing binary collisions. The solid-phase viscosity and pressure are determined as a function of granular temperature at any time and position.

The continuity equation for a generic phase q is given by following Equation:

$$\nabla \cdot (\alpha_q \rho_q \vec{v}_q) = 0 \quad (1)$$

Multiphase momentum conservation equation for a fluid phase q is given by Eq. (2):

$$\nabla \cdot (\alpha_q \rho_q \vec{v}_q \vec{v}_q) = -\alpha_q \nabla P + \nabla \cdot \bar{\tau}_q + \alpha_q \rho_q \vec{g} + K_{pq}(\vec{v}_s - \vec{v}_q) + \dot{m}_{sq} \vec{v}_{sq} - \dot{m}_{qs} \vec{v}_{qs} + (\vec{F}_q + \vec{F}_{lift,q} + \vec{F}_{vm,q}) \quad (2)$$

where, \vec{F}_q is an external body force, $\vec{F}_{\text{lift},q}$ is a lift force, $\vec{F}_{\text{vm},q}$ is a virtual mass force, K_{pq} is an interaction force between phases p and q, P is the pressure shared by all phases and $\bar{\tau}_q$ is the Newtonian stress tensor for fluid q. Phase q represents the real fluid and phase s represents the granular fluid.

A reciprocal momentum equation is written for granular fluid in Eq. (3):

$$\nabla \cdot (\alpha_s \rho_s \vec{v}_s \vec{v}_s) = -\alpha_s \nabla P + \nabla p_s + \nabla \cdot \bar{\tau}_s + \alpha_s \rho_s \vec{g} + K_{qs}(\vec{v}_q - \vec{v}_s) + \dot{m}_{qs} \vec{v}_{qs} - \dot{m}_{sq} \vec{v}_{sq} + (\vec{F}_s + \vec{F}_{\text{lift},s} + \vec{F}_{\text{vm},s}) \quad (3)$$

where, the solid-phase stresses $\bar{\tau}_s$ are derived by an analogy between the random particle motion arising from particle-particle collisions and the thermal motion of molecules in a gas, taking into account the inelasticity of the granular phase. The intensity of the particle velocity fluctuations determines the stresses, viscosity and pressure of the solid phase. The kinetic energy associated with the particle velocity fluctuations is represented by a granular temperature which is proportional to the mean square of the random motion of particles.

After preliminary tests, the lift force $\vec{F}_{\text{lift},s}$ and virtual mass force $\vec{F}_{\text{vm},s}$ were neglected since they gave a minor contribution to the solution compared to the other terms.

The solid-phase stress tensor is given by following equation:

$$\bar{\tau}_s = \alpha_s \mu_s (\nabla \vec{v}_s + \nabla \vec{v}_s^T) + \alpha_s \left(\lambda_s - \frac{2}{3} \mu_s \right) \nabla \cdot \vec{v}_s \bar{I} \quad (4)$$

where, the bulk viscosity of the solid-phase λ_s accounts for the resistance of the granular particles to compression and expansion. It has the following form according to Lun et al. (1984):

$$\lambda_s = \frac{4}{3} \alpha_s \rho_s d_s g_{0,s} (1 + e) \sqrt{\frac{\theta_s}{\pi}} \quad (5)$$

The fluid-solid momentum exchange coefficient uses Gidaspow et al. (1992) model as shown in Eq. (6):

$$K_{qs} = 150 \frac{\alpha_s (1 - \alpha_q) \mu_l}{\alpha_q d_s^2} + 1.75 \frac{\rho_q \alpha_s |\vec{v}_s - \vec{v}_q|}{d_s} \quad (6)$$

For multiple particle diameters, the exchange coefficient solid-solid is calculated from Eq. (7) by Syamlal (1987):

$$K_{qs} = \frac{3(1 + e_{s1s2}) \left(\frac{\pi}{2} + C_{fr,s1s2} \frac{\pi^2}{8} \right) \alpha_{s1} \rho_{s1} \alpha_{s2} \rho_{s2} (d_{s1} + d_{s2})^2 g_{0,s1s2} |\vec{v}_{s1} - \vec{v}_{s2}|}{2\pi(\rho_{s1} d_{s1}^3 + \rho_{s2} d_{s2}^3)} \quad (7)$$

The solid-phase pressure represents normal forces caused by particle-particle interactions and captures the effects on kinetic term in momentum transport caused by particle velocity fluctuations and a second term due to particle collisions, as shown in Eq. (8):

$$p_s = \alpha_s \rho_s \theta_s + 2\rho_s (1 + e_{ss}) \alpha_s^2 g_{0,ss} \theta_s \quad (8)$$

where, $g_{0,s}$ is the radial distribution function, which represents a correction factor that modifies the probability of collisions between particles when the solid granular phase becomes dense. The model present in ANSYS-Fluent modifies the equation from Ogawa et al. (1980) to determine the radial distribution for two or more solid phases.

The transport equation with granular temperature derived from GKT takes the form in the Eq. (9):

$$\frac{3}{2} \nabla \cdot (\rho_s \alpha_s \vec{v}_s \theta_s) = (-p_s \bar{I} + \bar{\tau}_s) : \nabla \vec{v}_s + \nabla \cdot (k_{\theta_s} \nabla \theta_s) - \frac{12(1 - e_s^2) g_{0s}}{d_s \sqrt{\pi}} \rho_s \alpha_s^2 \theta_s^{3/2} - 3K_{ls} \theta_s \quad (9)$$

where, $(-p_s \bar{I} + \bar{\tau}_s) : \nabla \vec{v}_s$ is the generation of energy by the solid stress tensor. The third and last terms on the right-hand-side represent the rate of energy dissipation within the solid-phase due to collisions between particles derived by Lun et al. (1984) and the transfer of the kinetic energy of random fluctuations in particles to fluid phase, respectively.

The diffusion coefficient for granular energy k_{θ_s} is given by Gidaspow et al. (1992) as:

$$k_{\theta_s} = \frac{150 d_s \rho_s \sqrt{\theta_s \pi}}{384(1 + e_{ss}) g_{0,ss}} \left[1 + \frac{6}{5} \alpha_s g_{0,ss} (1 + e_{ss}) \right]^2 + 2\rho_s \alpha_s^2 d_s (1 + e_{ss}) g_{0,ss} \sqrt{\frac{\theta_s}{\pi}} \quad (10)$$

The solid-phase stress tensor in Eq. (4) contains shear viscosity components shown in Eq. (11) arising from particle momentum exchange due to translation modelled by Syamlal et al. (1993) in Eq. (12) and collision modelled by Gidaspow et al. (1992) in Eq. (13). A frictional component of viscosity shown in Eq. (14) can also

be included to account for the viscous-plastic transition that occurs when particles of a solid phase reach the maximum solid volume fraction, as modelled by Johnson and Jackson (1987).

$$\mu_s = \mu_{s,col} + \mu_{s,kin} + \mu_{s,fr} \quad (11)$$

$$\mu_{s,kin} = \frac{\alpha_s \rho_s d_s \sqrt{\theta_s \pi}}{6(3 - e_s)} \left[1 + \frac{2}{5} (1 + e_s)(3e_s - 1) \alpha_s g_{os} \right] \quad (12)$$

$$\mu_{s,col} = \frac{4}{5} \alpha_s \rho_s d_s g_{os} (1 + e_s) \left(\frac{\theta_s}{\pi} \right)^{1/2} \quad (13)$$

$$\mu_{friction} = Fr \frac{(\alpha_s - \alpha_{s,min})^n}{(\alpha_{s,max} - \alpha_s)^p} \sin \emptyset \quad (14)$$

Where \emptyset is the angle of internal friction, with friction coefficient $Fr = 0.1\alpha_s$, $n=2$ and $p=5$ defined by Johnson and Jackson (1987).

The k- ϵ turbulence model offers a good compromise in terms of accuracy and robustness for general purpose simulations (Ofei and Ismail, 2016), using mixture properties and mixture velocities with empirical usual constants: $C_\mu=0.09$; $C_{1\epsilon}=1.44$; $C_{2\epsilon}=1.92$; $\sigma_k=1.0$ and $\sigma_\epsilon=1.3$.

The momentum exchange term for multiphase flows ($K_{qs}(\vec{v}_q - \vec{v}_s)$) in Eq. (3) corresponds to interphase turbulent momentum transfer due to turbulent drag and is modelled as shown in Eq. (14):

$$K_{qs}(\vec{v}_s - \vec{v}_q) = K_{qs}(\vec{U}_s - \vec{U}_q) + K_{qs} \left(\frac{D_s}{\sigma_{sq} \alpha_s} \nabla \alpha_s - \frac{D_q}{\sigma_{sq} \alpha_q} \nabla \alpha_q \right) \quad (14)$$

Where, $(\vec{U}_s - \vec{U}_q)$ is the difference of phase-weighted velocities. The last term corresponds to the drift velocity for each phase that results from turbulent fluctuations in the volume fraction, where D_s and D_q are diffusivity coefficients determined in Eq. (15), and σ_{sq} is the dispersion Prandtl number assumed as 0.75.

$$D_s = D_q = D_{t,sf} = \frac{1}{2} K_{qs} C_\mu \frac{k}{\epsilon} \sqrt{1 + (1.8 - 1.35 \cos^2 \theta) \left(\frac{(\vec{v}_s - \vec{v}_q) - \vec{v}_{dr}}{\sqrt{\frac{2}{3}} k} \right)^2} \quad (15)$$

3. Numerical Model

The pipe length of the model must be sufficiently long (Wasp et al.,1979) to ensure a statistically fully developed flow much anticipated to the outlet of the domain. The particles concentration will be reported within the fully developed flow region.

A uniform velocity and volume fraction of liquid and solid phases were introduced at the inlet, while an average pressure and zero-gradient velocity is prescribed at the outlet. Non-slip condition is established at walls.

The simulation used a second-order discretization in space, hexaedral unstructured O-grid mesh on halved pipe with vertical symmetry plane. Convergence was obtained when normalized residuals were smaller than $1e-05$ for all equations and with at least 0.75% global mass residual tolerance.

The mesh verification is performed over three meshes for a 3.00 m-long and 54.9 mm inner diameter horizontal pipe. The pressure drop was used as the verification parameter and a final mesh of 491,000 cells was chosen to further the study giving an error of less than 1% with respect to next coarser mesh.

4. Results

Kaushal et al. (2005) data were used to tune up granular temperature on the wall and to determine granular viscosity contribution for heterogeneous and saltation flow regimes.

The effect of wall granular temperature was assessed by considering either $1.0e-8 \text{ m}^2/\text{s}^2$ or $1.0e-5 \text{ m}^2/\text{s}^2$ values, since it dramatically affected the density of particles packed on the bottom of the pipe. Figure 1 shows the variation in bed concentration of up to 20% for the two adopted values using particles diameter of 0.440 mm. Results for the higher wall granular temperature depict a fairly accurate prediction, especially on the packed bed.

Figure 2 presents the effects of including or not the frictional contribution of the viscosity for the solid phase in the model. This figure shows the particle concentration for single particle diameter of 0.440 mm, bulk particle volumetric fraction of 10% and mean uniform inlet flow velocity of 2m/s. Results show that under the given conditions, non-inclusion of the frictional component of the solid-phase viscosity led to more accurate results.

Figure 3 shows the effect of the particle size (i.e. 0.125mm; 0.440mm and their combination) on the concentration distribution. As expected, smaller (lighter) particles are easily raised and depict a more homogeneous distribution than larger ones, which are dominated by gravity forces and accommodate in a heterogeneous pattern. The bi-disperse case depicts an intermediate behaviour between the observed conditions for individual sizes.

Figure 4 illustrates how the model reproduces the expected response when the inertial effects are increased further beyond the threshold that balances the gravity forces. Larger velocities, accordingly, depict a more homogeneous concentration, while the smaller velocities favour the sediments and thus, the heterogeneous regime. Strong bed particle packing, above 50%, observed at lowest mean velocity might need a deeper study of the frictional contribution of the solid viscosity.

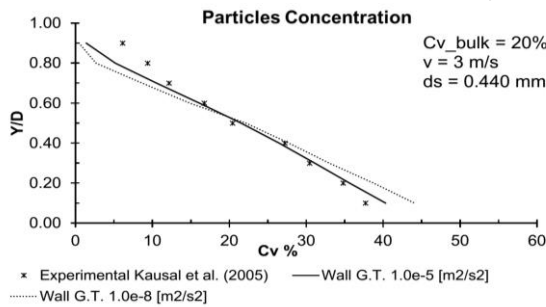


Figure 1: Effect of wall granular temperature on particle concentration

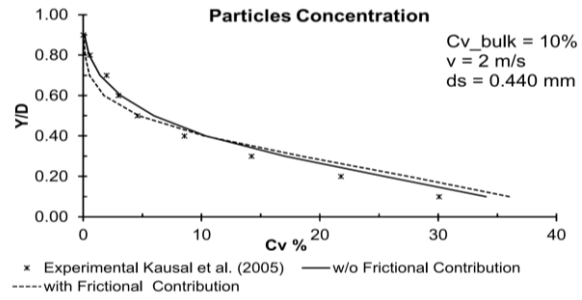


Figure 2: Effect of frictional contribution into solid-phase viscosity

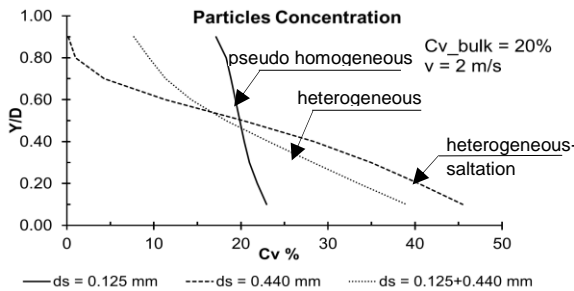


Figure 3: Incidence of particle size on concentration distribution

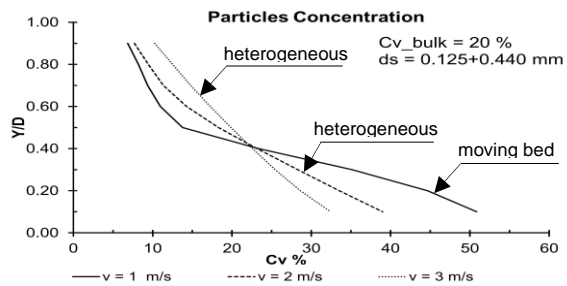


Figure 4: Incidence of mean inlet velocity on bi-disperse concentration distribution for particles of 0.440mm+0.125mm diameters

5. Concluding remarks

The predicting capability of a multiphase numerical model to reproduce the transport of particles in slurry flows is assessed under effects of flow regime, monodisperse and bi-disperse liquid-particle flow, mixture velocity and particles bulk concentration. An Eulerian-Eulerian model using the Granular Kinetic Theory is developed to treat the dispersed solid phase as a fluid with collisional, kinetic and frictional contributions into its viscosity. Preliminary tune-up of the model is performed based on evaluation of sensible wall granular temperature and frictional component of solid viscosity.

The wall granular temperature proved to be a very important element in the modelling. In fact, tuning its value permits to control the level of particle agitation near the wall and therefore, affects the prediction of near-wall concentration. The bi-disperse mixture depicts a hybrid behaviour as the cross concentration of particles tend to adopt an intermediate distribution between that observed for individual particles.

Larger particles show an important response to gravitational force, as expected, and play a primary role in the determination of cross-section concentration profiles. Turbulence carrying capacity is appreciated above a threshold value of the velocity, for which small/mid particles are easily transported by the fluid, turning the flow into a homogeneous slurry mixture.

Nomenclature

α or C_v	Volume concentration	k_{θ_s}	Diffusion coefficient	θ_s	Granular temperature
$\alpha_{s,max}$	Solid maximum packing	K_{ls}	Momentum exchange coefficient	μ	Dynamic viscosity
C_D	Drag coefficient	λ	Bulk viscosity	$\mu_{s,col}$	Collisional viscosity
d_s	Diameter of particle	p_s	Solid Pressure	$\mu_{s,kin}$	Kinetic viscosity
e_s	Restitution coefficient	$P_{frictio}$	Frictional pressure	$\mu_{s,fr}$	Frictional viscosity
\vec{g}	Gravity vector	Re_s	Relative Reynolds number	\vec{v}	Velocity
g_{os}	Radial distribution function	ρ	Density	θ_s	Granular temperature
γ_{θ_s}	Particle collisions dissipation	$\bar{\tau}$	Stress tensor		

References

- Chemloul N., Chaib K., Mostefa K., 2009, Simultaneous measurements of the solid particles velocity and concentration profiles in two phase flow by pulsed ultrasonic doppler velocimetry, J. of the Braz. Soc. of Mech. Sci.&Eng., 31, 333-343
- Durand R., and Condolios E., 1952, Experimental investigation of the transport of solids in pipes, Deuxieme Journée de l'hydraulique, Societé Hydrotechnique.
- Ekambara K., Sanders R.S., Nandakumar K., Masliyah J.H., 2009, Hydrodynamic simulation of horizontal slurry pipeline flow using ANSYS-CFX, Ind. Eng. Chem. Res., 48, 8159-8171.
- Gidaspow D., Bezburuah R., Ding J., 1992, Hydrodynamics of circulating fluidized beds: Kinetic theory approach, 7th Engineering Foundation International Conference on Fluidization, 75-82.
- Gillies R.G., Shook C.A., 2000, Modeling high concentration settling slurry flows, Canadian Journal of Chemical Engineering, Vol. 78, 709-716.
- Hernández F., Blanco A., Rojas-Solórzano L., 2008, CFD modeling of slurry flow in horizontal pipes, Symposium on Applications in Computational Fluid Dynamics, 8, FEDSM2008-55103.
- Hu, S., 2006, Multiphase Flow Handbook, Clayton T. Crowe Ed., Chapter 4.
- Johnson P.C., Jackson, R., 1987, Frictional-collisional constitutive relations for granular materials, with application to plane shearing. J. Fluid Mech., Vol. 176, 67-93.
- Kaushal D.R., Sato K., Toyota T., Funatsu K., Tomita Y., 2005, Effect of particle size distribution on pressure drop and concentration profile in pipeline flow of highly concentrated slurry, International Journal of Multiphase Flow, 31, 809-823.
- Kaushal D.R., Thinglas T., Tomita Y., Kuchii Sh., Tsukamoto H., 2012, CFD modeling for pipeline flow of fine particles at high concentration, International Journal of Multiphase Flow, 43, 85-100.
- Kumar A., Kanwarpal, Singh B., 2015, CFD modeling for silica sand slurry in horizontal pipeline system, YMCAUST International Journal of Research, 3, ISSN: 2319-9377.
- Ling J., Skudarnov P.V., Lin C.X., Ebadian M.A., 2003, Numerical investigations of liquid–solid slurry flows in a fully developed turbulent flow region, International Journal of Heat and Fluid Flow, 24, 389-398.
- Lun C.K.K., Savage S.B., Jeffrey D.J., Chepurniy N., 1984, Kinetic Theories for Granular Flow: Inelastic particles in Couette flow and slightly inelastic particles in a general flow field, J. Fluid Mech., 140, 223-256.
- Newitt, M., Richardson F., Abbott, M. Turtle, B., 1955, Hydraulic conveying of solids in horizontal pipes, Trans Inst. of Chem. Eng., 33, 93-113.
- Ofei T.N., Ismail A.Y., 2016, Eulerian-Eulerian simulation of particle-liquid slurry flow in horizontal pipe, Journal of Petroleum Engineering, ID: 574371.
- Ogawa S., Umemura A., Oshima N., 1980, On the equations of fully fluidized granular materials, J. Applied Mathematics and Physics (ZAMP), 31, 483-492.
- Polansky J., 2014, Experimental investigation of slurry flow, Investice do Rozvoje Vzdelavani, CZ.1.07/2.3.00/20.0139.
- Syamlal M., 1987, The particle-particle drag term in a multiparticle model of fluidization, National Technical Information Service, DOC/MC/21353-2373, NTIS/DE87006500.
- Syamlal M., Rogers W., O'Brien T. J., 1993, MFIX Documentation/Theory Guide, Technical Note, US Department of Energy, DOE/METC-94/1004 (DE94000087).
- Thomas D. G., 1964, Transport characteristics of suspensions, Chem. Eng. Journal, 10, 303–308.
- Wasp E.J., Aude T.C., Kenny J.P., Seiter R.H., Jacques, R.B., 1970, Deposition velocities transition velocities and spatial distribution of solids in slurry pipelines, BHRA Fluid Engineering, 42, 53-76.
- Wasp E.J., Kenny J.P., Gandhi R.L., 1979. Solid–Liquid Flow: Slurry Pipeline Transportation, Gulf Publishing Co, Houston, Texas.
- Wilson K.C., Pugh F.J., 1988, Dispersive-force modelling of turbulent suspension in heterogeneous slurry flow, Can. J. Chem. Eng., Vol. 66, 721-727.